Journal of Magnetism and Magnetic Materials 456 (2018) 217–222

Contents lists available at ScienceDirect

Journal of Magnetism and Magnetic Materials

journal homepage: www.elsevier.com/locate/jmmm

Research articles

Thermopower and magnetocaloric properties in NdSrMnO/CrO_3 composites

A.M. Ahmed [a], H.F. Mohamed [a,*], J.A. Paixão [b], Sara A. Mohamed [a]

[a] Physics Department, Faculty of Science, Sohag University, 82524 Sohag, Egypt
[b] CFisUC, Department of Physics, University of Coimbra, P-3004-516 Coimbra, Portugal

ARTICLE INFO

Article history:
Received 23 November 2017
Received in revised form 26 January 2018
Accepted 12 February 2018
Available online 13 February 2018

ABSTRACT

The thermoelectric power (TEP) and magnetocaloric effect (MCE) for $(Nd_{0.6}Sr_{0.4}MnO_3)_{1-x}/(CrO_3)_x$ composites have been measured. The TEP measurements show a negative sign value of the Seebeck coefficient (*S*), in microvolts. TEP data construe in the low range of temperature by the magnon and phonon drag model, whereas at high temperature by small polaron conduction mechanism. Magnetic measurements exhibit that all composites show a paramagnetic–ferromagnetic transition with decreasing temperature. The Arrott plots of composites reveal the occurrence of a second order phase transition. The maximum value of magnetic entropy change (ΔS) is 2.37 J kg^{-1} K^{-1}, achieved fore the composite with $x = 0.015$. Moreover, the maximum value of relative cooling power (RCP) is 122.1 J kg^{-1}, achieved for the composite with $x = 0.020$. These composites may be appropriate for magnetic application near room temperature.

1. Introduction

The strong connection of the different kinds of transport properties of manganites is responsible for their high sensitivity to external factors such as temperature, magnetic field and pressure. Two reasons make these materials of great relevance. Firstly, the TEP materials can recover waste heat and transform it to electrical current through the Seebeck effect (S) [1,2]

The conversion efficiency of this process is determined through the figure of merit (ZT) dimensionless factor ($ZT = S^2\rho^{-1}\kappa^{-1}T$, where ρ is the electrical resistivity, κ is the thermal conductivity and T is the absolute temperature. Secondly, extensive research work in manganites [3–4] shows that these materials can be used in magnetic cooling technology. Magnetic refrigeration is a new cooling technology based on the magnetocaloric effect (MCE), which is occurred in these materials to achieve enormously low temperatures. The main idea of magnetic cooling can be summarizes as follows: when a magnetic field is applied adiabatically to a magnetic material, the unpaired spins are align parallel to the field. The magnetic entropy of the material is lowered and the sample warms up recovering the lost magnetic entropy through the increase of its lattice entropy. on the other hand, when the magnetic field is removed from the sample, the spins tends to randomize, increasing the magnetic entropy and lowering both the lattice entropy and the temperature of the material. Both the TEP and the MCE arise due to the presence of two sources of energy in magnetic materials, phonon and magnon excitations. Interaction between these two degrees of freedom are normally coupled with the spin lattice coupling.

One of the typical simple manganites systems is $Nd_{0.6}Sr_{0.4}MnO_3$ (NSMO) composite. Magnetic, electrical properties of these materials can be investigated by changing temperature, pressure, annealing temperature and various cation dopants [5,6]. This system recorded a small S with a metallic behavior (μV range) and it was n-type as many oxides. From an applied point of view, large *S* and n-type thermo elements are required.

A Previous report [7] showed that the effect of adding CrO_3 on the NSMO matrix increases the resistivity and decreases the metal-semiconductor transition (T_{ms}). On the other side, magnetization measurements revealed almost unchanged in Curie temperature (T_c), also a drop in the magnetic moment. The irregular change in T_c is due to magnetic reduction which comes from the replacement of the Cr^{3+} ion for Mn^{3+} ion weakens the double exchange (DE) [8].

The influence of heat treatment on $Nd_{0.6}Sr_{0.4}MnO_3$ composition was reported in Ref. [9]. It elucidated that the NSMO system exhibit FM-PM transitions at a certain temperature. Also the annealing process improves magnetic entropy (ΔS) and the relative cooling power (RCP) of NSMO compound, where ΔS and RCP recorded the highest value at T_{an} = 700 & 900 °C respectively. From our point of view, there's little study on the effect of adding CrO_3 on the TEP and the MCE of the $Nd_{0.6}Sr_{0.4}MnO_3$ composites. So, in this

* Corresponding author.
E-mail addresses: h.fathy@science.sohag.edu.eg, dr_hanyfathy@yahoo.com (H.F. Mohamed).

https://doi.org/10.1016/j.jmmm.2018.02.037
0304-8853/

manuscript, we will investigate the effect of adding CrO_3 on the TEP and the MCE properties.

2. Experimental procedure

$(Nd_{0.6}Sr_{0.4}MnO_3)_{1-x}/(CrO_3)_x$ composites with x = 0, 0.005, 0.010, 0.015, 0.020, 0.025&0.030 wt% were prepared by the conventional solid-state reaction method as reported in [7]. Thermoelectric power measurements were carried out in previous reports [10,11]. The magnetic measurements were carried out using aDynacool/Quantum Design Physical Properties Measuring System (PPMS). In an isothermal process of magnetization, the total magnetic entropy change of the system due to the application of a magnetic field, ΔS_M, can be determined from the thermo- dynamic Maxwell relation $(dS/dH)_T = (dM/dT)_H$ [12] by means of

$$DS_M = S_M(T,H) - S_M(T,0) = \int_0^H (dM(T,H)/dT)_H dH \quad (1)$$

Thus, numerical integration of two smoothed consecutive isothermal M(H) curves around mean temperature $T = 1/2(T_{i+1}+T_i)$ allow us to approximately determine $\Delta S_M(T,H)$ [13] by

$$\Delta S_M = S_M(T,H) - S_M(T,0) = \int_0^H (dM(T,H)/dT)_H dH \quad (2)$$

An appropriate parameter often used to explain the potential of magnetocaloric materials is the relative cooling power (RCP) [14] which is defined by

$$RCP = |\Delta S|_{max} \Delta T_{FWHM} \quad (3)$$

where $|\Delta S|_{max}$ is the maximum value of magnetic entropy change and ΔT_{FWHM} is the full width at half maximum of the peak in the entropy change.

3. Results and discussions

3.1. Structural properties

The X-ray and Rietveld refinement technique indicates that all composites are a single orthorhombic phase and there are no CrO_3 grains separated as Ref. [7]. It was observed from the scanning electron microscope (SEM) images that the grain boundaries are clear and no any trace of CrO_3. This pointed to the CrO_3 goes into the perovskite lattice and/or perhaps a little part of the Cr_2O_3 is in the grain boundaries [7].

Table 1
The best fit parameters obtained from thermoelectric power data for $(Nd_{0.6}Sr_{0.4}MnO_3)_{1-x}/(CrO_3)_x$ system with $(0 \le x \le 0.03)$.

x. (at%)	So(μV/K)	S1(μV/K)	S3/2(μV/K)	S3(μV/K)	S4(μV/K)
0	−7.9	0.19	−0.01	-6.29×10^{-7}	2.63×10^{-9}
0.005	56.93	−2.98	0.29	-6.8×10^{-5}	1.63×10^{-7}
0.010	−46.86	2.19	−0.21	4.23×10^{-5}	-8.99×10^{-8}
0.015	−47.46	2.19	−0.21	4.23×10^{-5}	-8.99×10^{-8}
0.020	−72.01	3.73	−0.36	6.65×10^{-5}	-1.23×10^{-7}
0.025	75.56	−3.24	0.29	-5.47×10^{-5}	-1.15×10^{-7}
0.030	76.16	−3.25	0.29	-5.47×10^{-5}	1.15×10^{-7}

3.2. Thermoelectric power (TEP)

3.2.1. TEP as function of temperature

Fig. 1 shows the temperature dependence of the Seebeck coefficient S for the composites. S values are in Micro-volts for all composites with a negative sign overall the temperature range. This indicates that the conduction is governed only by intrinsic charge carriers of electrons, which are thermally excited from valence

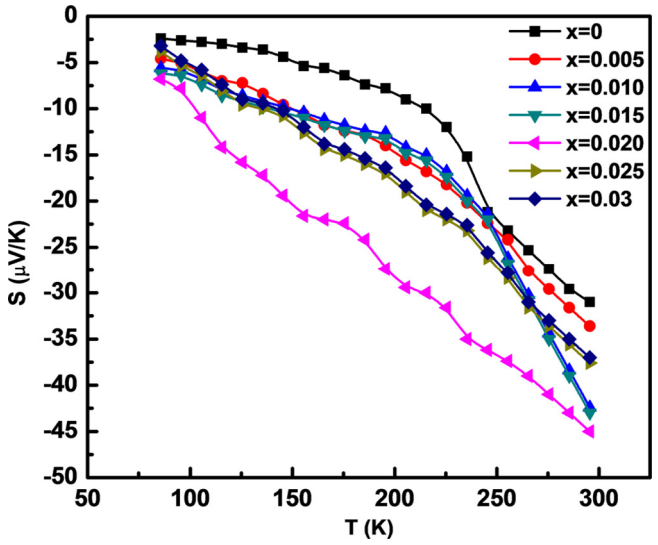

Fig. 1. S versus T of $(Nd_{0.6}Sr_{0.4}MnO_3)_{1-x}/(CrO_3)_x$, where $(0 \le x \le 0.03)$.

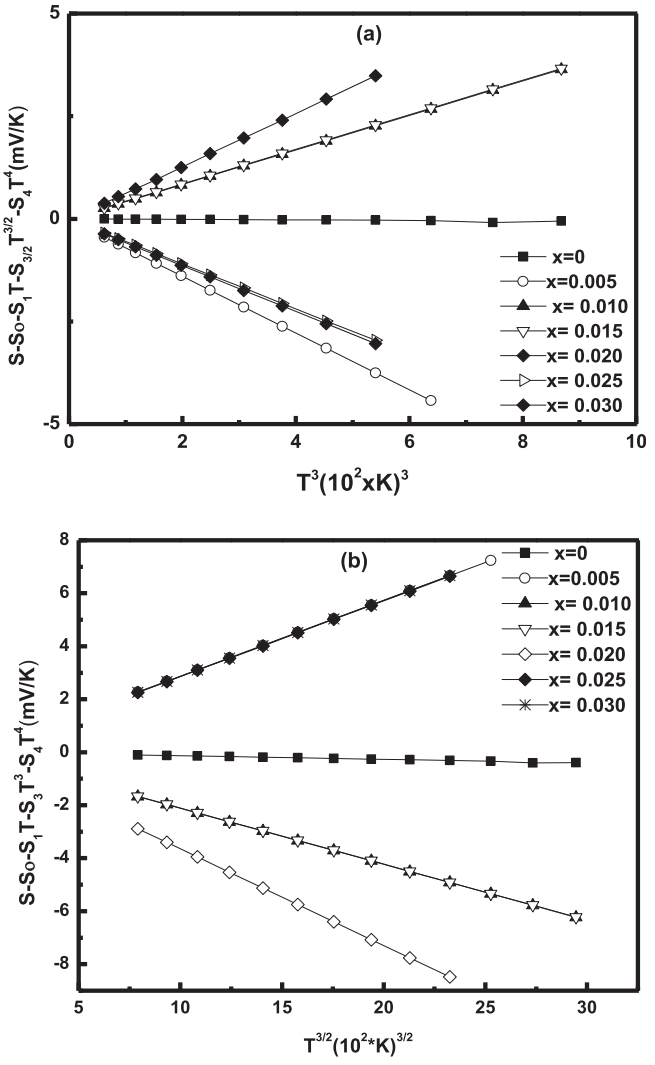

Fig. 2. (a) The phonon drag behavior dependent on (T^3), (b) the magnon drag behavior dependent on $T^{3/2}$ of $(Nd_{0.6}Sr_{0.4}MnO_3)_{1-x}/(CrO_3)_x$.

Table 2
The thermopower activation energy E_s, the parameter α, T_S(K) and the small polaron hopping energy W_H.

x. (at%)	TS(K)	Es(meV)	α	Eρ(meV) [11]	WH(meV)
0	215	18.150	−1082.92	137.51	119.4
0.005	215	15.034	−975.80	165.11	150.1
0.010	225	27.5	−1562.41	146.78	119.2
0.015	225	30.223	−1682.03	141.89	111.7
0.020	235	11.788	−982.89	141.89	203.6
0.025	245	16.74	−1094.45	140.44	123.7
0.030	175	16.961	−1102.36	181.87	164.9

band into conduction band. All composites show a peak in $S(T)$ at temperature (T_s) representing the metal- semiconductor transition [15]. The T_s value increases with Cr content as listed in Table 1, and it is found to be greater than the T_{ms} values determined from electrical resistivity measurements [7]. This suggests a relation between carriers band width and mobility when the composites are cooled towards T_{ms}. This alters the slope in the $S(T)$ curves at T_s [16,17] and the spin wave theory has been incorporated to analyze the temperature dependence of S in low temperature region.

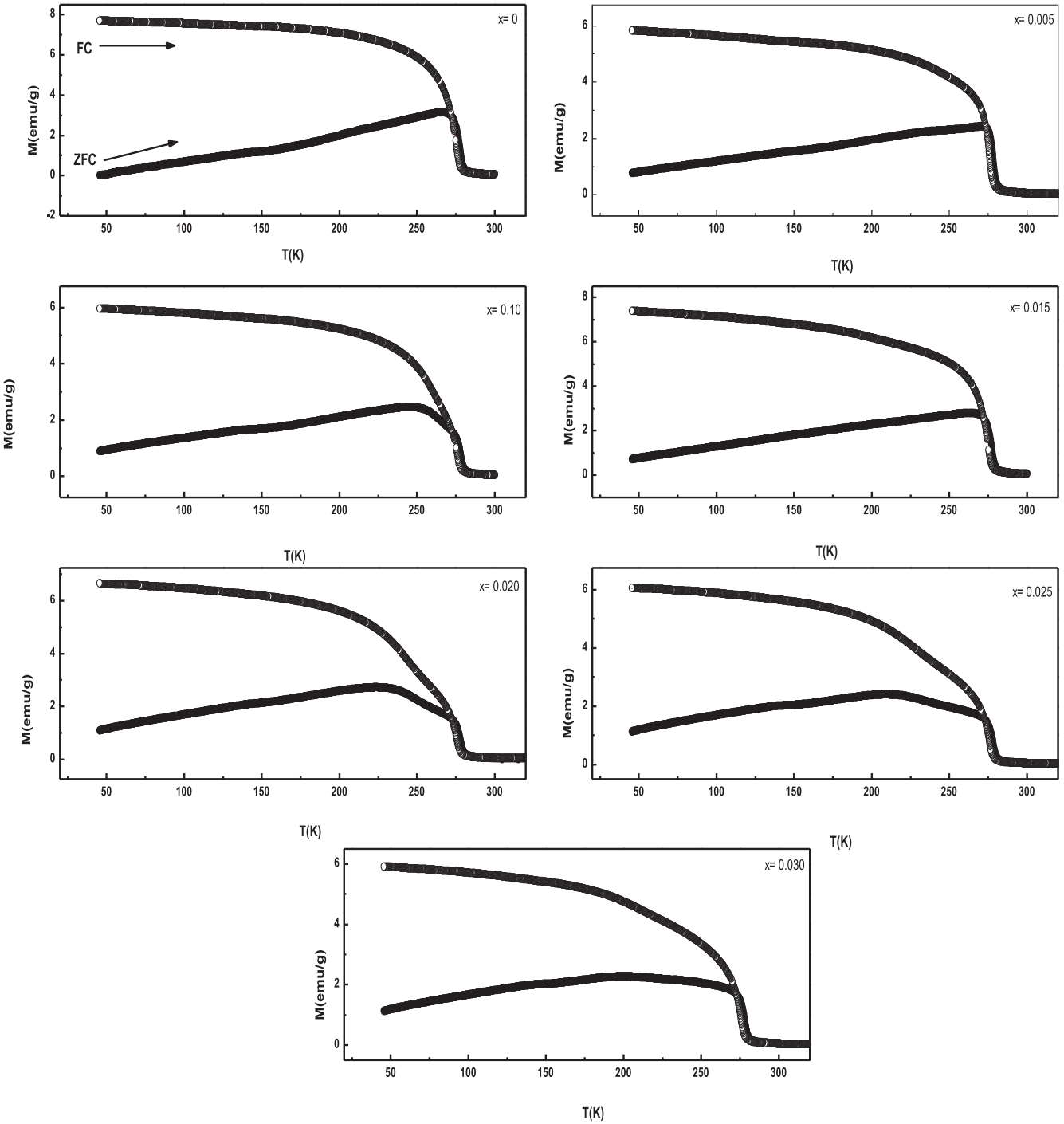

Fig. 3. Field cooled and zero field cooled magnetization of bulk of $(Nd_{0.6}Sr_{0.4}MnO_3)_{1-x}/(CrO_3)_x$ as a function of temperature, measured in the field ranges of 100 Oe.

Table 3
Curie temperature T_C, the temperature represents the onset of canting T_p, and/or random freezing of the spins and maximum entropy measured at 3 T for analyzed samples.

x. (at%)	0	0.005	0.010	0.015	0.020	0.025	0.030
T_c(K)	276	278	278	275	278	278	278
T_p(K)	–	–	–	–	230	210	200
$\Delta S_{M(max)}$ (J/kg.K)	1.84	1.71	1.79	2.37	1.65	1.33	1.53

3.2.2. Low temperature behavior

In the low temperature region, both magnon drag (S_m) and phonon drag (S_g) contribute along the diffusion (S_d) [18,19]. The magnon drag effect is created owing to the presence of electron–magnon scattering, while the phonon drag is due to electron–phonon scattering. The whole S–T range depicted in Fig. 2 was analysed using the following relation [19] (note that $n_{ph} \propto T^3$, $n_{mag} \propto T^{3/2}$):

$$S = S_\circ + S_1 T + S_{3/2} T^{3/2} + S_3 T^3 + S_4 T^4 \quad (4)$$

where, S_o (S at $T = 0$) is a constant, $S_{3/2}T^{3/2}$ is due to the electron – magnon scattering, S_3T^3 term is due to phonon drag and S_4T^4 is due to spin wave fluctuation.

Results in Table 1 show that $S_{3/2} > S_3$ which indicates the dominance of electron-magnon scattering. There are other mechanisms behind the phonon- electron drag contribution such as magnon drag, impurities and spin wave fluctuation. The phonon drag effect on thermopower decreases at lower temperature where it vanishes at 0 K.

3.2.3. High temperature behavior

The conduction process at high temperatures (paramagnetic phase) in manganites is due to thermal activated polarons [20–22]. Hence S is given by the well known Mott's equation [23]

$$S = \pm\left(\frac{k_B}{e}\right)\left[\frac{E_s}{k_B T} + \alpha\right] \quad (5)$$

where E_s is the activation energy, α is a constant. When $\alpha < 1$ the hopping is due to small polaron, but if $\alpha > 2$ the hopping is due to a large polaron. As seen in Table 2, $\alpha < 1$, which is the case of the small polaron hopping. Also, it is noteworthy the lower value of

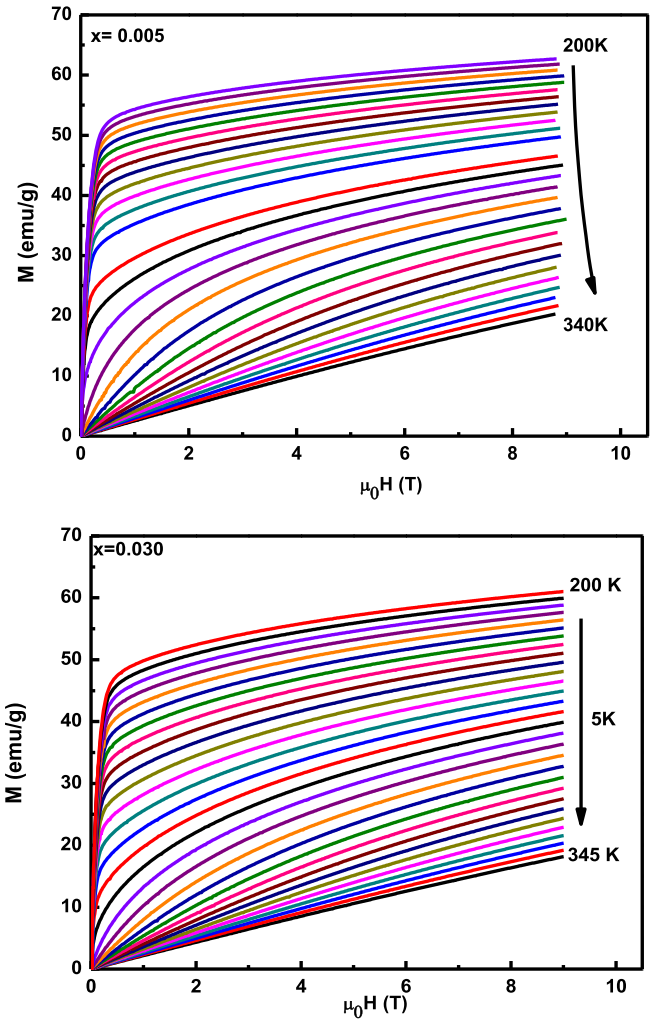

Fig. 4. Isothermal specific magnetization M(H) curves for $(Nd_{0.6}Sr_{0.4}MnO_3)_{0.995}/(CrO_3)_{0.005}$ & $(Nd_{0.6}Sr_{0.4}MnO_3)_{0.97}/(CrO_3)_{0.03}$.

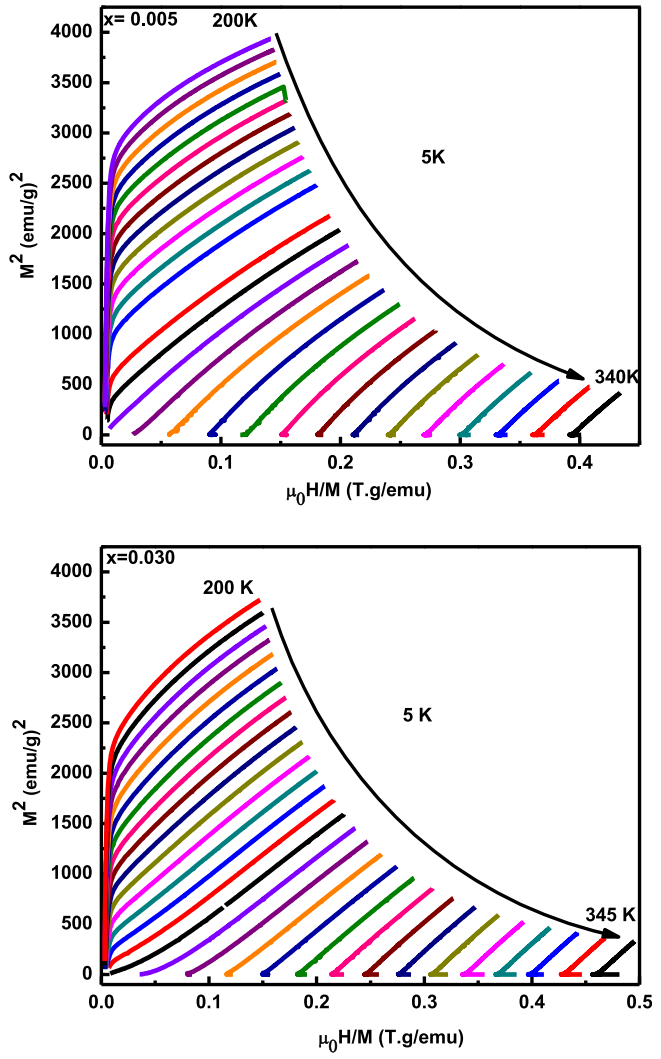

Fig. 5. M^2 versus $\mu_0 H/M$ determined from the magnetization isotherms for $x = 0.005$& 0.03 composites.

E_s incomparison with E_a obtained from electrical measurements reported in [7], which supports the SPH conduction [18].

3.2.4. Magnetic properties and magnetocaloric effect (MCE)

The temperature dependences of zero-field-cooled $M_{ZFC}(T)$ and field-cooled $M_{FC}(T)$ of $(Nd_{0.6}Sr_{0.4}MnO_3)_{1-x}/(CrO_3)_x$ composites under H = 100 Oe are shown in Fig. 3. It is observed that $M_{ZFC}(T)$ increases with increasing temperature up to T_c for $x \leq 0.015$ whereas M_{FC} decreases slowly. For $x \geq 0.020$ composites show a cusp at certain temperature T_p in ZFC magnetization curves (see Table 3). The T_p, represents the onset of canting and/or random freezing of the spins, where the magnetization decreases with the decrease of temperature. In the case of $x \geq 0.020$ samples, maybe there are a small impurity phases (didn't appear in XRD) responsible for clusters like behavior, is clearly indicated by the cusp in the ZFC curve

Additionally, we observed that all composites are creating a bifurcation between FC and ZFC curves in the ferromagnetic region. The observed difference between these curves may be due to short range ferromagnetic clusters, owing to the presence of low Sr ionic concentration at Nd site. One other hand, the low field $M_{ZFC/FC}(T)$ curves reveal strong irreversibility for $T \leq T_C$. As in Table 3 the value of T_c remains almost unchanged but the T_p decreases with further CrO_3 content for $x \geq 0.020$.

The isothermal magnetization curves were measured and Fig. 4 shows those of $x = 0.005$ and x = 0.030 composites as examples. Magnetization in curves below T_c increases rapidly at $H < 0.5\ T$ then tendes to saturation at $H > 0.5\ T$, which confirms the ferromagnetic behavior. Fig. 5 shows the Arrott plots (M^2 versus $\mu_0 H/M$) determined from the magnetization isotherms for $x = 0$, 0.05&0.03 samples. The curves clearly show a positive slope for the complete M^2 range, which confirm the occurence of a second order phase transition [24]. The T_c values deduced from Arrott plots are in agreement with those obtained from the $M(T)$ ones.

ΔS_M as a function of temperature for a field variation from 0 to H_{max} is given by a more abrupt variation of magnetization near the magnetic transition occurs and results in large magnetic entropy. Fig. 6 shows the temperature dependences of ΔS_M (T, H) for $(Nd_{0.6}Sr_{0.4}MnO_3)_{1-x}/(CrO_3)_x$ composites at different values of magnetic field up to 3 T. As shown in Fig. 6, ΔS_M shows negative values with a maximum around the T_C for all composites. This maximum increases with increasing applied magnetic field. Also $\Delta S_{M\ (max)}$ shifts towards higher temperature and increases in amplitude with increasing magnetic fields. The transition peak of ΔS_M is very broad in all composites this due to the second-order nature of the phase transition. Conversely, for compounds featuring a first order magnetic transition, a sharp narrower maximum is observed due to the considerable variation of magnetization near T_C [25]. Despite of the irregular change in ΔS_M, the composite with $x = 0.015$ shows the highest value of 2.37(J/kg.K) at $H = 3\ T$ (see Table 3).

The relative cooling power (RCP) is determined from equation:

$$RCP = |\Delta S|_{max} \Delta T_{FWHM} \quad (6)$$

where $|\Delta S|_{max}$ and ΔT_{FWHM} is the maximum value of magnetic entropy change and the full width at half maximum of the peak, respectively. Fig. 7 shows the RCP values for all composites. The RCP increases with the CrO_3 content and reaches a maximum value of 122.1 J kg^{-1} for the $x = 0.020$ composite at 3 T applied magnetic field. The results of ΔS_M and RCP of these composites evidently suggest that they are high enough for technical interest. The large magnetic entropy changes in manganite originates from the abrupt reduction of magnetization, which is related with a FM-PM phase transition near the Curie temperature. The parameters ΔS_M (J/kg.K), T_C and RCP for composites are comparable to the values found in other NSMO compounds as in Table 4. The present system has a T_C near to room temperature

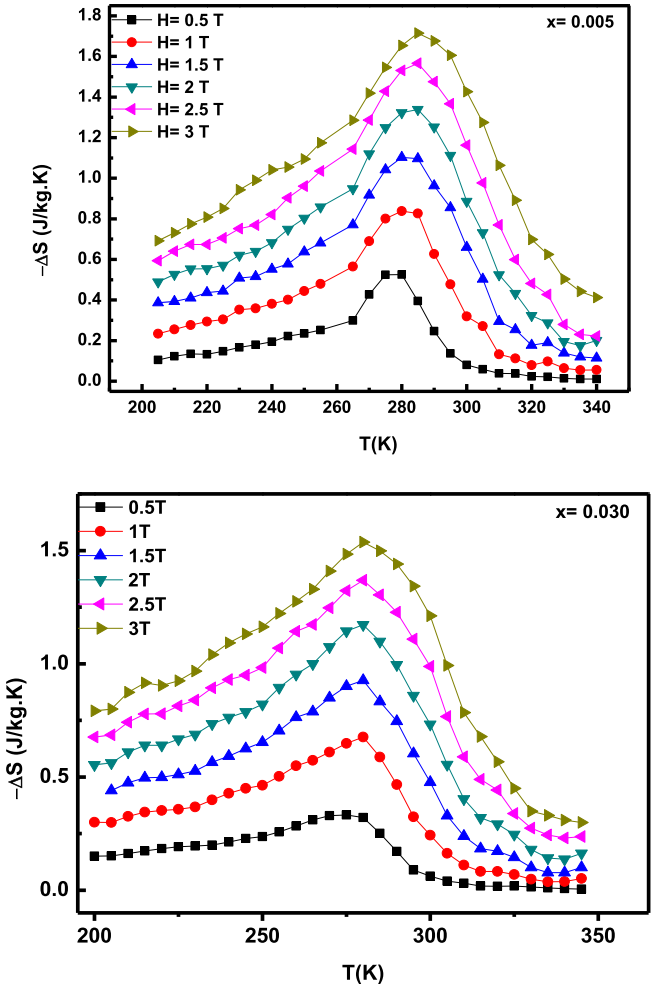

Fig. 6. Temperature dependences of the magnetic entropy change for x = 0.005 & 0.03 composites.

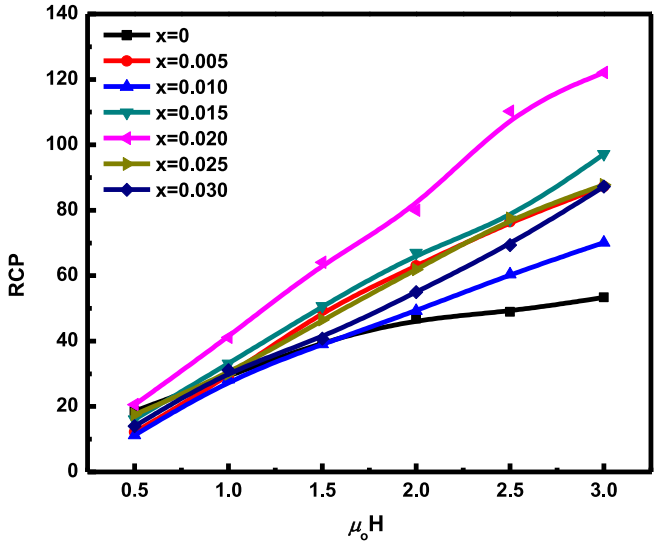

Fig. 7. Relative cooling power values RCP as a function of applied magnetic field (H) for $(Nd_{0.6}Sr_{0.4}MnO_3)_{1-x}/(CrO_3)_x$ composites.

Table 4
Comparison of maximum entropy change, Curie temperature, and *RCP* for $Nd_{0.6}Sr_{0.4}MnO_3$ and other NSMO compounds.

Sample	T_C(K) Heating	ΔH(T)	$\|\Delta S\|^{max}$[J/kg.K]	RCP[J/kg]	Ref
$(Nd_{0.6}Sr_{0.4}MnO_3)_{0.98}/(CrO_3)_{0.02}$	278	3	1.65	122.1	Present work
$(Nd_{0.6}Sr_{0.4}MnO_3)_{0.975}/(CrO_3)_{0.025}$	278	3	1.33	87.78	Present work
$(Nd_{0.6}Sr_{0.4}MnO_3)_{0.97}/(CrO_3)_{0.03}$	278	3	1.53	87.21	Present work
$Nd_{0.6}Sr_{0.4}MnO_3$	272	2	1.8	38	[13]
$Nd_{0.7}Sr_{0.3}MnO_3$	240	2	5.3	80	[5]
$Nd_{0.7}Sr_{0.3}MnO_3$	203	1.4	3.8	–	[26,27]
$Nd_{0.5}Sr_{0.5}MnO_3$	150	1.4	10.5	–	[26]
$Nd_{0.7}Sr_{0.3}MnO_3$	155	1.35	1.9	15	[28]

4. Conclusion

The thermoelectric power and magnetic properties of polycrystalline $(Nd_{0.6}Sr_{0.4}MnO_3)_{1-x}/(CrO_3)_x$ composites were examined. The values of S are in the micro-volt range and have a negative sign for all temperature range. All composites have a peak represent the transition temperature (T_s) determined from thermopower data due to metal-semiconductor transition. The analysis of $S(T)$ in the low temperature region illustrated both S_m and the S_g contribute with S_d. On the other side, the values of E_s are lower than E_ρ, which confirmed the SPH mechanism. The $M_{ZFC/FC}(T)$ measurements show that M_{ZFC} increases with increasing temperature up to T_c for $x \leq 0.015$, but M_{FC} decreases. All composites are creating a divergence between FC and ZFC curves in the ferromagnetic region.

Our results show that CrO_3 addition affects the magnetocaloric properties, shifting the maximum value of the ΔS_M towards lower temperatures. Furthermore, it is observed that CrO_3 doping increases both T_c and T_s.

Acknowledgments

This work was partially supported by funds from FEDER (Programa Operacional Factores de Competitividade COMPETE) and from FCT-Fundação para a Ciência e a Tecnologia under the Project No. UID/FIS/04564/2016. Access to TAIL-UC facility funded under QREN-Mais Centro Project No. ICT_2009_02_012_1890 is gratefully acknowledged.

References

[1] H. Kuwahara, Y. Hirobe, J. Nagayama, S. Kodama, A. Kakishima, J. Magn. Magn. Mater. 272 (2004) e1393.
[2] A.M. Ahmed, A. Kattwinkel, K. Barner, C.P. Yang, J.R. Sun, G.H. Rao, Physica B 324 (2002) 102–109.
[3] Abd El-Moez A. Mohamed, V. Vega, M. Ipatov, A.M. Ahmed, B. Hernando, J. All. Comp. 665 (2016) 394e403
[4] R. M'nassri, A. Cheikhrouhou, J. Supercond. Nov. Magn. 27 (2014) 1463–1468
[5] The-Long Phan, T.A. Ho, P.D. Thang, Q.T. Tran, T.D. Thanh, N.X. Phuc, M.H. Phan, B.T. Huy, S.C. Yu, J. All. Comp. 615 (2014) 937–945.
[6] T. GeethaKumary, S.L. Cheng, J.G. Lin, J. Appl. Phys. 101 (2007) 093910.
[7] A.M. Ahmed, H.F. Mohamed, A.K. Diab, S.A. Mohamed, Indian J. Phys. 91 (2) (2017) 169–181.
[8] M. Eshraghi, P. Kameli, H. Salamati J. Theoret, Appl. Phys. 7 (2013) 1.
[9] A.M. Ahmed, H.F. Mohamed, A.K. Diab, Sara A. Mohamed, S. García-Granda, D. Martínez-Blanco, Solid State Sci. 57 (2016) 1e8
[10] A.M. Ahmed, G. Papavassiliou, H.F. Mohamed, E.M.M. Ibrahim, J. Magn. Magn. Mater. 392 (2015) 27–41.
[11] A.M. Ahmed, Physica B 352 (2004) 330–336.
[12] A.M. Tishin, Y.I. Spichkin, The Magnetocaloric Effect Manganits Applications, Institute of Physics, 2003, p. 17.
[13] J. Fan, L. Ling, B. Hong, L. Pi, Y. Zhang, J. Magn. Magn. Mater 321 (2009) 2838.
[14] Pedro Gorria, Jos eL Sanchez Llamazares, PabloAlvarez, María Jos ePerez1, Jorge Sanchez Marcos, Jesús A. Blanco, J. Phy. D Appl. Phy. 41 (2008) 192003.
[15] S. Bhattacharya, A. Banerjee, S. Pal, R.K. Mukherjee, B. K. chaudhuri, J. Appl. Phys. 93 (2003) 356–361.
[16] N. Rama, V. Sankaranarayan, M.S. Ramachandra Rao, J. All. Comp. 466 (2008) 12–16
[17] P. Mandal, Phys. Rev. B 61 (2000) 14675.
[18] S. Battacharya, S. Pal, A. Banerjee, H.D. Yang, B.K. Chaudhuri, J. Chem. Phys. 119 (2003) 3972.
[19] B.H. Kim, J.S. Kim, T.H. Park, D.S. Le, Y.W. Park, J. Appl. Phys. 103 (2008) 113717.
[20] J.M.D. Coey, J.M.D, M. Viret, S. von Molnar, Adv. Phys. 48 (1999) 167–293.
[21] G.J. Snyder, R. Hiskes, S. Dicarolis, M.R. Beasley, T.H. Geballe, Phys. Rev. B 53 (1996) 14434.
[22] J.D. Lee, B.I. Min, Phys. Rev. B 55 (1997) 12454.
[23] N.F. Mott, Davis, Electronics process in Non crystalline Materials, Clarendon, Oxford, 1979.
[24] N.K. Singh, K.G. Suresh, A.K. Nigam, Solid State Commun. 127 (2003) 373–377.
[25] N.S. Bingham, M.H. Phan, H. Srikanth, M.A. Torija, C. Leighton, J. Appl. Phys. 106 (2009) 023909.
[26] R. Venkatesh, K. Sethupathi, M. Pattabiraman, G. Rangarajan, J. Magn. Magn. Mater. 310 (2007) 2813.
[27] R. Venkatesh, M. Pattabiraman, S. Angappane, G. Rangarajan, K. Sethupathi, J. Karatha, M. Fecioru-Morariu, R.M. Ghadimi, G. Guntherodt, Phys. Rev. B 75 (2007) 224415.
[28] N. Chau, D.H. Cuong, N.D. Tho, H.N. Nhat, N.H. Luong, B.T. Cong, J. Magn. Magn. Mater. 1292 (2004) 272.